

Time and Frequency Domain Methods for Basis Selection in Random Linear Dynamical Systems

John D. Jakeman*, Roland Pulch†

July 7, 2021

Abstract

Polynomial chaos methods have been extensively used to analyze systems in uncertainty quantification. Furthermore, several approaches exist to determine a low-dimensional approximation (or sparse approximation) for some quantity of interest in a model, where just a few orthogonal basis polynomials are required. We consider linear dynamical systems consisting of ordinary differential equations with random variables. The aim of this paper is to explore methods for producing low-dimensional approximations of the quantity of interest further. We investigate two numerical techniques to compute a low-dimensional representation, which both fit the approximation to a set of samples in the time domain. On the one hand, a frequency domain analysis of a stochastic Galerkin system yields the selection of the basis polynomials. It follows a linear least squares problem. On the other hand, a sparse minimization yields the choice of the basis polynomials by information from the time domain only. An orthogonal matching pursuit produces an approximate solution of the minimization problem. We compare the two approaches using a test example from a mechanical application.

Keywords. linear dynamical system, random variable, orthogonal basis, polynomial chaos, stochastic Galerkin method, least squares problem, orthogonal matching pursuit, uncertainty quantification

1 Introduction

We consider linear dynamical systems in the form of ordinary differential equations (ODEs), which include physical parameters. A quantity of interest (QoI) is defined as an output of the system. Uncertainties may be present in the parameters. In uncertainty quantification, a common approach is to interpret the parameters as random variables, see [1, 2].

The state variables as well as the QoI can be expanded into a series with given orthogonal basis polynomials depending on the random variables and a priori unknown time-dependent coefficient functions. This spectral approach is called a (generalized) polynomial chaos expansion, see [3, 4, 1, 2]. Several types of numerical methods exist to compute an approximation of the coefficient functions. On the one hand, the stochastic Galerkin method projects the random linear dynamical system to a larger deterministic linear system of ODEs, whose solution yields the approximation, see [5, 6]. On the other hand, the approximation can be fitted to random samples in a least squares regression, see [7].

The number of basis polynomials up to a given total degree becomes huge in the case of a large number of random variables. Our task is to identify a low-dimensional approximation of the random QoI, which is sometimes called a sparse representation in the literature. Therein, just a small subset of basis polynomials is required for a sufficiently accurate approximation. Numerical methods for this problem were based on least angle regression [8], sparse grid quadrature [9], compressed sensing [10, 11], and reduced basis techniques [12, 13], for example. Dimension-adaptive ANOVA decompositions [14, 15, 16], and low-rank tensor approximations [17, 18] can also be used to address the curse-of-dimensionality.

In this paper, the aim is to further explore numerical methods for low-dimensional representations. We investigate and compare two techniques to construct a low-dimensional approximation with q basis

Disclosure: See acknowledgements

Correspondence author: Roland Pulch (roland.pulch@uni-greifswald.de)

*Center for Computing Research, Sandia National Laboratories, P.O. Box 5800, MS 1318, Albuquerque, NM, 87185-1320, United States.

†Institute of Mathematics and Computer Science, University of Greifswald, Walther-Rathenau-Straße 47, D-17489 Greifswald, Germany.

polynomials, where q is a given integer number. Both approaches fit their approximations to a set of samples from the QoI in the time domain. First, a frequency domain analysis is performed for the transfer function of the stochastic Galerkin system, which was derived in the previous work [19]. The minimization of an error bound identifies a subset of q basis polynomials. We apply this subset and identify the accompanying time-dependent coefficient functions by a least squares problem, which was not considered in [19]. In addition, we examine an ℓ_0 -minimization under a constraint purely in the time domain, which also yields a subset of q basis polynomials. Orthogonal matching pursuit (OMP) [20] generates a numerical approximation to the minimization problem.

We apply both techniques to a test example, which models a mass-spring-damper system with random parameters. A comparison of the errors for the low-dimensional approximations is presented. Moreover, we examine the conformance of both approaches, i.e., if the techniques predominantly identify the same basis polynomials.

2 Problem Definition

The problem of the basis selection is specified in this section. We denote the sets of real numbers and complex numbers by \mathbb{R} and \mathbb{C} , respectively.

2.1 Linear dynamical systems

In this section we investigate linear dynamical systems of the form

$$\begin{aligned} E(p)\dot{x}(t, p) &= A(p)x(t, p) + B(p)u(t) \\ y(t, p) &= C(p)x(t, p), \end{aligned} \quad (1)$$

where the matrices $A, E \in \mathbb{R}^{n \times n}$, $B \in \mathbb{R}^{n \times n_{\text{in}}}$ and $C \in \mathbb{R}^{n_{\text{out}} \times n}$ depend on physical parameters $p \in \Pi \subseteq \mathbb{R}^{n_{\text{par}}}$. An input $u : [0, \infty) \rightarrow \mathbb{R}^{n_{\text{in}}}$ is given and an output $y : [0, \infty) \times \Pi \rightarrow \mathbb{R}^{n_{\text{out}}}$ is provided. Without loss of generality, we restrict the investigations to the case of single-input-single-output (SISO), i.e., $n_{\text{in}} = n_{\text{out}} = 1$.

We assume that the mass matrix E is always non-singular. Consequently, a system of ODEs (1) is given with the state variables $x : [0, \infty) \times \Pi \rightarrow \mathbb{R}^n$. In our examinations, initial value problems (IVPs) $x(0, p) = 0$ are predetermined for all $p \in \Pi$. Furthermore, we assume that the systems (1) are asymptotically stable for all $p \in \Pi$, i.e., all eigenvalues $\Sigma(p) \subset \mathbb{C}$ of the matrix pencil $\lambda E(p) - A(p)$ have a negative real part.

The input-output mapping of the system (1) can be specified by a transfer function $H : (\mathbb{C} \setminus \Sigma(p)) \rightarrow \mathbb{C}$ in the frequency domain, see [21, p. 65]. The transfer function of the system (1) becomes

$$H(s, p) := C(p)(sE(p) - A(p))^{-1}B(p) \quad \text{for } s \in \mathbb{C} \setminus \Sigma(p), \quad (2)$$

which represents a rational function in the frequency variable s . The input-output mapping reads as $Y(s, p) = H(s, p)U(s)$, where U, Y denote the Laplace transforms of the input and the output, respectively.

2.2 Stochastic modeling and orthogonal basis

In the dynamical system (1), the parameters $p \in \Pi$ are replaced by independent random variables $p : \Omega \rightarrow \Pi$ on some probability space $(\Omega, \mathcal{A}, \mu)$ with event space Ω , sigma-algebra \mathcal{A} and probability measure μ . We suppose the existence of a joint probability density function $\rho : \Pi \rightarrow \mathbb{R}$. Given a measurable function $f : \Pi \rightarrow \mathbb{R}$, the expected value reads as

$$\mathbb{E}[f] := \int_{\Omega} f(p(\omega)) \, d\mu(\omega) = \int_{\Pi} f(p)\rho(p) \, dp$$

provided that the integral is finite. The associated Hilbert space

$$\mathcal{L}^2(\Pi, \rho) := \{f : \Pi \rightarrow \mathbb{R} : f \text{ measurable and } \mathbb{E}[f^2] < \infty\}$$

features the inner product

$$\langle f, g \rangle := \mathbb{E}[fg] = \int_{\Pi} f(p)g(p)\rho(p) \, dp \quad \text{for } f, g \in \mathcal{L}^2(\Pi, \rho). \quad (3)$$

The norm of the Hilbert space reads as

$$\|f\|_{\mathcal{L}^2(\Pi, \rho)} := \sqrt{\langle f, f \rangle}. \quad (4)$$

In the system (1), we assume that $x_1(t, \cdot), \dots, x_n(t, \cdot), y(t, \cdot) \in \mathcal{L}^2(\Pi, \rho)$ point-wise for $t \in [0, \infty)$.

We consider an orthonormal system $(\Phi_i)_{i \in \mathbb{N}} \subset \mathcal{L}^2(\Pi, \rho)$ consisting of polynomials. The theory of the generalized polynomial chaos (gPC) applies in this situation, see [22, 2]. Hence the basis functions satisfy the orthogonality relations

$$\langle \Phi_i, \Phi_j \rangle = \begin{cases} 0 & \text{for } i \neq j, \\ 1 & \text{for } i = j. \end{cases} \quad (5)$$

Such an orthonormal system exists under the above assumptions. However, the system is not always complete, cf. [4]. Since we investigate finite approximations, completeness is not required in the following.

Finite approximations are obtained by

$$x^{(m)}(t, p) = \sum_{i=1}^m v_i(t) \Phi_i(p) \quad \text{and} \quad y^{(m)}(t, p) = \sum_{i=1}^m w_i(t) \Phi_i(p) \quad (6)$$

including m basis polynomials. Due to the orthogonalities (5), the transient coefficient functions $v_i : [0, \infty) \rightarrow \mathbb{R}^n$ and $w_i : [0, \infty) \rightarrow \mathbb{R}$ given by

$$v_{i,j}(t) = \langle x_j(t, \cdot), \Phi_i(\cdot) \rangle \quad \text{and} \quad w_i(t) = \langle y(t, \cdot), \Phi_i(\cdot) \rangle \quad (7)$$

represent the best approximation in the subspace spanned by $\{\Phi_1, \dots, \Phi_m\}$ with respect to the norm (4). If the orthonormal system is complete, then the convergence

$$\lim_{m \rightarrow \infty} \left\| y(t, \cdot) - y^{(m)}(t, \cdot) \right\|_{\mathcal{L}^2(\Pi, \rho)} = 0 \quad \text{for each } t$$

is guaranteed for the output (QoI) and, likewise, for the state variables.

We assume that the orthonormal system $(\Phi_i)_{i \in \mathbb{N}}$ is ordered in ascending total degrees, i.e., $\text{degree}(\Phi_i) \leq \text{degree}(\Phi_j)$ for $i \leq j$. Thus $\Phi_1 \equiv 1$ is the unique constant polynomial. Let the approximation (6) include all polynomials up to a total degree d . The number of polynomials reads as, see [2, p. 65],

$$m(d) = \frac{(n_{\text{par}} + d)!}{n_{\text{par}}! d!} \quad (8)$$

for a fixed number n_{par} of random parameters. This number becomes large for high dimensions n_{par} of the random space, even though the total degree may be moderate, say $2 \leq d \leq 5$.

2.3 Stochastic Galerkin method

We investigate the input-output behavior of a stochastic Galerkin system.

2.3.1 Stochastic Galerkin system and transfer function

An approximation of the coefficient functions (7) belonging to the solution of the random dynamical system (1) can be obtained by a stochastic Galerkin approach. This technique yields a larger coupled system

$$\begin{aligned} \hat{E} \dot{\hat{v}}(t) &= \hat{A} \hat{v}(t) + \hat{B} u(t) \\ \hat{w}(t) &= \hat{C} \hat{v}(t) \end{aligned} \quad (9)$$

with matrices $\hat{A}, \hat{E} \in \mathbb{R}^{mn \times mn}$, $\hat{B} \in \mathbb{R}^{mn}$ and $\hat{C} \in \mathbb{R}^{m \times mn}$. Thus the system is single-input-multiple-output (SIMO). The matrix \hat{E} is non-singular in most cases and thus (9) is a system of deterministic ODEs. Although the stochastic Galerkin system may be unstable, see [23], this loss of stability happens rather seldom. We assume that the system (9) is asymptotically stable. IVPs $\hat{v}(0) = 0$ are imposed. More details on the stochastic Galerkin approach for random linear dynamical systems can be found in [5, 6, 19].

The outputs $\hat{w} = (\hat{w}_1, \dots, \hat{w}_m)^\top$ of the system (9) represent an approximation of the exact coefficients (7). The associated approximation of the QoI in the random dynamical system (1) reads as

$$\hat{y}^{(m)}(t, p) = \sum_{i=1}^m \hat{w}_i(t) \Phi_i(p). \quad (10)$$

The Galerkin-projected system (9) exhibits its own input-output behavior described by a complex-valued transfer function $\hat{H} : \mathbb{C} \setminus \hat{\Sigma} \rightarrow \mathbb{C}$, $\hat{H} = (\hat{H}_1, \dots, \hat{H}_m)^\top$ with a finite set of poles $\hat{\Sigma}$, see [24, 25]. It holds that

$$\hat{H}(s) = \hat{C} (s\hat{E} - \hat{A})^{-1} \hat{B} \quad \text{for } s \in \mathbb{C} \setminus \hat{\Sigma}. \quad (11)$$

Again the transfer function represents a rational function. The linear dynamical system (9) is asymptotically stable, if and only if the set of poles $\hat{\Sigma}$ is located in the left half of the complex plane. Moreover, the transfer function is always strictly proper for systems of ODEs, which is defined by the condition

$$\lim_{s \rightarrow \infty} \hat{H}(s) = 0 \quad (12)$$

in each component. The computational effort for an evaluation of (11) is dominated by a single LU -decomposition of the matrix $s\hat{E} - \hat{A}$.

In the frequency domain, Hardy norms characterize the magnitude of a transfer function, see [21]. These norms allow for error estimates. We will use the \mathcal{H}_2 -norm component-wise, i.e.,

$$\|\hat{H}_i\|_{\mathcal{H}_2} = \sqrt{\frac{1}{2\pi} \int_{-\infty}^{+\infty} |\hat{H}_i(i\omega)|^2 d\omega} = \sqrt{\frac{1}{\pi} \int_0^{+\infty} |\hat{H}_i(i\omega)|^2 d\omega} \quad (13)$$

for $i = 1, \dots, m$ with $i = \sqrt{-1}$. Alternatively, the \mathcal{H}_∞ -norm can be considered component-wise, i.e.,

$$\|\hat{H}_i\|_{\mathcal{H}_\infty} = \sup_{\omega \in \mathbb{R}} |\hat{H}_i(i\omega)| = \sup_{\omega \geq 0} |\hat{H}_i(i\omega)| \quad (14)$$

for $i = 1, \dots, m$. In [19], both \mathcal{H}_2 - and \mathcal{H}_∞ -norm were investigated in this context. We apply only the \mathcal{H}_2 -norm in the following, because the results are qualitatively the same in both cases.

2.3.2 Computation of Hardy norms

There are several possibilities to compute the \mathcal{H}_2 -norm of a linear dynamical system, cf. [21]. We use an own technique based on quadrature, where the computational effort is nearly independent of the number m of basis polynomials. An approximation of the \mathcal{H}_2 -norms (13) is obtained by a quadrature with (single) rectangular rule in $[0, \omega_{\min}]$ and composite trapezoidal rule in $[\omega_{\min}, \omega_{\max}]$ given $0 < \omega_{\min} < \omega_{\max}$. We apply a grid of the form $\omega_{\min} = \omega_1 < \omega_2 < \dots < \omega_{\nu-1} < \omega_\nu = \omega_{\max}$. The approximation of (13) reads as

$$\int_0^\infty |\hat{H}_i(i\omega)|^2 d\omega \approx \omega_1 |\hat{H}_i(i\omega_1)|^2 + \sum_{j=2}^\nu \frac{\omega_j - \omega_{j-1}}{2} \left(|\hat{H}_i(i\omega_{j-1})|^2 + |\hat{H}_i(i\omega_j)|^2 \right)$$

for $i = 1, \dots, m$. Since the transfer function (11) is continuous at $\omega = 0$, the quadrature error within $[0, \omega_{\min}]$ is negligible for ω_{\min} sufficiently close to zero. The property (12) guarantees that the truncation error, which arises by discarding the interval (ω_{\max}, ∞) , is negligible for sufficiently large ω_{\max} . In each node of the quadrature, the evaluation of (11) requires mainly an LU -decomposition of the matrix $i\omega_j \hat{E} - \hat{A}$ independent of the output matrix \hat{C} provided that m is not extremely large.

2.3.3 Applicability to differential-algebraic equations

If the mass matrix $E(p)$ is singular, then the linear dynamical system (1) consists of differential-algebraic equations (DAEs). In most cases, the mass matrix \hat{E} of the stochastic Galerkin system (9) also becomes singular. We assume an asymptotically stable system (9) again, where the set of poles $\hat{\Sigma}$ is situated in the left

half of the complex plane. It follows that the associated matrix pencil is regular. We outline the potential to obtain the frequency domain information from Section 2.3.1, which is required for the basis selection in Section 2.5.

A linear system of DAEs is characterized by its (nilpotency) index $\kappa \in \mathbb{N}$ ($\kappa \geq 1$), see [26, p. 454]. Let κ be the index of the stochastic Galerkin system (9). Consequently, the transfer function of (9) reads as

$$\hat{H}(s) = \hat{H}_{\text{SP}}(s) + \hat{P}(s) \quad (15)$$

with a strictly proper vector-valued rational function \hat{H}_{SP} satisfying (12) and a vector-valued polynomial \hat{P} of degree at most $\kappa - 1$. The formula (15) is valid for DAEs in general, see [27]. If the polynomial part \hat{P} vanishes, then the \mathcal{H}_2 -norms (13) do exist for all components. Hence the strategy performs as in the case of ODEs. If the polynomial part does not vanish, then some or all \mathcal{H}_2 -norms do not exist.

If the index of the stochastic Galerkin system (9) is one, then the polynomial part \hat{P} becomes constant (degree zero). In this case, the existence of the \mathcal{H}_∞ -norms (14) is guaranteed for all components. The frequency domain analysis can be done using the norms (14).

2.4 Basis selection and low-dimensional representations

Let an initial approximation (6) be given with a large number (8) of basis polynomials up to total degree d . Let $\mathcal{I}^d := \{1, \dots, m(d)\}$ be the respective index set. In general, nearly all associated coefficient functions are non-zero. However, the coefficients typically exhibit different orders of magnitudes and a fast decay for increasing degree.

Our aim is to identify a low-dimensional representation

$$\tilde{y}^{(\mathcal{I})}(t, p) = \sum_{i \in \mathcal{I}} \tilde{w}_i(t) \Phi_i(p) \quad (16)$$

with an index set $\mathcal{I} \subset \mathcal{I}^d$ satisfying $q := |\mathcal{I}| \ll m(d)$. Thus the selected basis functions from (16) represent a subset of the basis functions in (6). Yet the difference $y - \tilde{y}^{(\mathcal{I})}$ with y from (1) or (at least) $\hat{y}^{(m(d))} - \tilde{y}^{(\mathcal{I})}$ with \hat{y} from (10) should be sufficiently small in the $\mathcal{L}^2(\Pi, \rho)$ -norm point-wise in time. The approximation (16) is also called a q -sparse representation, cf. [8] for a motivation. Hence the problem consists in the identification of both the index set \mathcal{I} and associated approximations \tilde{w}_i of the coefficient functions for a desired number q . If a transient solution of the stochastic Galerkin system (9) is available, then we can simply set $\tilde{w}_i := \hat{w}_i$ for $i \in \mathcal{I}$.

2.5 Analysis in frequency domain

In [19], the error $\hat{y}^{(m(d))} - \tilde{y}^{(\mathcal{I})}$ between the approximation (10) from the stochastic Galerkin method and the low-dimensional approximation (16) was analyzed using the frequency domain. The \mathcal{H}_2 -norms (13) of the transfer function belonging to the Galerkin-projected system (9) are considered. Let $\mathcal{I} \subset \mathcal{I}^d$ be any index set. Theorem 1 in [19] demonstrates the error estimate

$$\sup_{t \geq 0} \left\| \hat{y}^{(m(d))}(t, \cdot) - \tilde{y}^{(\mathcal{I})}(t, \cdot) \right\|_{\mathcal{L}^2(\Pi, \rho)} \leq \sqrt{\sum_{i \in \mathcal{I}^d \setminus \mathcal{I}} \left\| \hat{H}_i \right\|_{\mathcal{H}_2}^2} \|u\|_{\mathcal{L}^2[0, \infty)} \quad (17)$$

with $\tilde{w}_i = \hat{w}_i$ for all $i \in \mathcal{I}$. The usual $\mathcal{L}^2[0, \infty)$ -norm is used for the time-dependent input. An advantage is that the error is bounded uniformly for all times. However, this error bound is not sharp.

For a desired cardinality $q = |\mathcal{I}|$, we determine a minimum upper bound in the right-hand side of (17). An optimal index set satisfies, see [19, p. 7],

$$\mathcal{I}_q = \arg \min_{\mathcal{I} \subseteq \mathcal{I}^d} \left\{ \sum_{i \in \mathcal{I}^d \setminus \mathcal{I}} \left\| \hat{H}_i \right\|_{\mathcal{H}_2}^2 : |\mathcal{I}| = q \right\}. \quad (18)$$

In practice, the norms will be pairwise different. Hence the unique index set \mathcal{I}_q includes the components with the q largest \mathcal{H}_2 -norms. Furthermore, the minimization of the upper bound is independent of the

choice of the input u . Approximations of the \mathcal{H}_2 -norms, which occur in (18), can be computed numerically as described in Section 2.3.2.

This frequency domain analysis can be extended to the case of multiple outputs ($n_{\text{out}} > 1$) in (1) straightforward. Either a large output matrix $\hat{C} \in \mathbb{R}^{m n_{\text{out}} \times mn}$ in (9) or n_{out} separate systems (9) with output matrices $\hat{C}_j \in \mathbb{R}^{m \times mn}$ for $j = 1, \dots, n_{\text{out}}$ can be arranged. We discuss the latter approach. In the transfer function (11), the part

$$\hat{F}(s) := (s\hat{E} - \hat{A})^{-1}\hat{B}$$

is identical for any output. An evaluation of $\hat{F}(i\omega)$ can be reused for all systems in a quadrature to approximate the integrals (13). Thus the computational effort for a frequency domain analysis is nearly independent of the number of outputs (provided that $n_{\text{out}} \ll mn$). A separate low-dimensional basis can be computed for each output.

3 Numerical Methods

In this section, we discuss numerical techniques for a computation of a low-dimensional representation and its coefficient functions in the time domain. Specifically, we consider two approaches: (i) sparsity inducing regression and (ii) least squares regression using the sparse index set consisting of the q largest Hardy norms identified by the frequency domain analysis.

3.1 Sampling techniques

Our numerical methods apply the information from k samples of the output (QoI) of the linear dynamical system (1) for realizations p_1, \dots, p_k of the random variables. We collect the samples in a vector-valued time-dependent function

$$\bar{y}(t) := (y(t, p_1), \dots, y(t, p_k))^{\top}. \quad (19)$$

Let a basis $\{\Phi_1, \dots, \Phi_{m(d)}\}$ be given with all orthonormal polynomials up to a total degree d . We arrange the Vandermonde matrix

$$V \in \mathbb{R}^{k \times m}, \quad V = (v_{ij}), \quad v_{ij} := \Phi_j(p_i) \quad (20)$$

for $i = 1, \dots, k$ and $j = 1, \dots, m$. This matrix is dense. Now let $v_1, \dots, v_m \in \mathbb{R}^k$ be the columns of the matrix (20) and $\mathcal{I}_q \subseteq \mathcal{I}^d$ with $\mathcal{I}_q = \{j_1, \dots, j_q\}$ be an arbitrary subset of indices. We use the notation

$$V_{\mathcal{I}_q} := (v_{j_1}, \dots, v_{j_q}) \in \mathbb{R}^{k \times q} \quad (21)$$

for the matrix, which consists of the associated subset of columns from the Vandermonde matrix (20). The cardinality (8) of the total-degree basis $m(d)$ grows quickly with the number of random parameters n_{par} and degree d . Thus, in the following, we assume $k < m(d)$, because for computationally expensive linear dynamical systems we cannot afford to run the model exhaustively.

3.2 Orthogonal matching pursuit

We consider the determination of a sparse representation in the time domain now.

3.2.1 Algorithm

Let a fixed time point $t > 0$ be given. We use OMP [20] to determine a q -sparse representation at this time point by greedily minimizing the ℓ_0 -norm

$$\|w\|_0 := |\{i : w_i \neq 0\}| \quad \text{for } w \in \mathbb{R}^m,$$

which counts the number of non-zero entries in a vector. Specifically, the OMP approach finds an approximation to the problem

$$\tilde{w}(t) = \arg \min \|\tilde{w}(t)\|_0 \quad \text{such that} \quad \|V\tilde{w}(t) - \bar{y}(t)\|_2 \leq \varepsilon \quad (22)$$

with the Euclidean norm $\|\cdot\|_2$ and $\varepsilon \geq 0$ by iteratively building up an approximation of the solution vector $\tilde{w}(t)$. At each iteration step, a least squares problem is solved using a subset of active columns of V . At the q th iteration step, OMP updates an active index set \mathcal{I}_q , in a greedy fashion, such that the inactive column index $j \notin \mathcal{I}_q$ with the highest correlation (inner product) with the current residual is added to the active set. This update reads as

$$\mathcal{I}_q = \mathcal{I}_{q-1} \cup \{j\} \quad \text{with} \quad j = \arg \max_{i \in \mathcal{I} \setminus \mathcal{I}_{q-1}} \frac{r_{q-1}(t)^\top v_i}{\|v_i\|_2}. \quad (23)$$

OMP then solves the least squares problem

$$\arg \min_{\tilde{w}^{(q)}(t) \in \mathbb{R}^q} \|r_q(t)\|_2, \quad (24)$$

where $r_q(t) = V_{\mathcal{I}_q} \tilde{w}^{(q)}(t) - \bar{y}(t)$.

Setting $\varepsilon = 0$ in (22), the algorithm yields a finite sequence of q -sparse approximations (16) for $q = 1, 2, \dots, q_{\max}$, where $q_{\max} \leq \min(k, m)$, thus removing the need to estimate ε . In the following, we will assume that $q_{\max} \leq k < m$, which always implies over-determined linear systems. For a given number q the solution obtained using OMP is a greedy attempt to find a solution with q non-zero coefficients such that the residual

$$R(t) := \|V\tilde{w}(t) - \bar{y}(t)\|_2 \quad (25)$$

is minimal. We will employ this approach in the time domain.

Unlike the least squares approach in Section 3.3, OMP must be applied at each time point separately. Here we use an OMP implementation based upon rank-one updates of a QR -factorization of the matrix $V_{\mathcal{I}_q}$ to form $V_{\mathcal{I}_{q+1}}$, see [28, p. 334]. The total complexity of the q th iteration is $O(km + ks)$. As shown in [29], the total complexity of our OMP for a single time point is

$$q_{\max} km + m \sum_{q=1}^{q_{\max}} q = m q_{\max} \left(k + \frac{1}{2}(q_{\max} + 1) \right).$$

OMP does not require the construction of the full Vandermonde matrix. If memory is limited, one can simply compute each basis vector v_i for $i \in \mathcal{I} \setminus \mathcal{I}_{q-1}$ in each iteration $q = 1, \dots, q_{\max}$. The construction of the basis vector v_i is necessary to compute the inner products $r_{q-1}(t)^\top v_i$ and $\|v_i\|_2$ in (23). Although the full Vandermonde matrix does not have to be stored, the QR -factorization of the matrix $V_{\mathcal{I}_q}$ must be stored. Only if $q = m$, then $V_{\mathcal{I}_q}$ will be the full Vandermonde matrix. However, we suppose $q \ll m$.

Note that avoiding the storage of the full Vandermonde matrix requires repeated computation of the basis vectors v_i , which affects the complexity analysis. For the problem sizes considered in this paper memory was not an issue, so the full Vandermonde matrix was stored to avoid the redundant computation of the basis vectors.

3.2.2 Theoretical guarantees

OMP is directly related to ℓ_1 -minimization [30] which finds the dominant gPC coefficients by solving

$$\tilde{w}(t) = \arg \min \| \tilde{w}(t) \|_1 \quad \text{such that} \quad \| V \tilde{w}(t) - \bar{y}(t) \|_2 \leq \varepsilon \quad (26)$$

with the norm $\|w\|_1 = |w_1| + \dots + |w_m|$ for $w \in \mathbb{R}^m$. This ℓ_1 -minimization problem is often referred to as Basis Pursuit Denoising. The problem obtained by setting $\varepsilon = 0$, to enforce interpolation, is termed Basis Pursuit (BP).

Let $\{\Phi_1, \dots, \Phi_m\}$ be an orthonormal polynomial basis with respect to the probability measure of the random variables p , i.e., the relations (5) are satisfied. Furthermore, in (26), let $V \in \mathbb{R}^{k \times m}$ be the matrix obtained by random sampling the basis under the probability measure. If the number of samples k satisfies

$$k \geq CL_m q \log^3 q \log m \quad \text{with} \quad L_m = \max_{i=1, \dots, m} \|\Phi_i\|_\infty^2,$$

then every q -sparse vector can be recovered by (26) (for $\varepsilon = 0$) with probability at least $1 - m^{-\gamma \log^3 q}$ including constants $C, \gamma > 0$, see [31]. The maximum norm $\|\cdot\|_\infty$ is taken over the support of the probability measure.

OMP requires stronger theoretical conditions than BP, see [32]. For example, for a sufficiently small ratio of the number of samples to sparsity, BP can guarantee recovery of all q -sparse polynomials with high probability, whereas, for a fixed set of samples, OMP can guarantee recovery of at least one sparse polynomial but not all, see [33]. However, despite this theoretical difference, in practice OMP can still obtain comparable accuracy to non-approximate algorithms such as BP [33]. Moreover, OMP has a much faster execution speed than most algorithms, which in conjunction with its iterative nature makes OMP more amenable to assessing the effect of sparsity on the accuracy of our approximations for dynamical systems.

We remark that although we focus on linear problems, sparse approximation strategies can also be applied to nonlinear dynamical systems, for example [7].

3.3 Least squares problem

Orthogonal matching pursuit greedily builds up a sparse representation of the output (QoI) of a linear dynamical system (1) and uses least squares to solve an over-determined linear system. Alternatively, we determine a q -sparse representation applying a basis specified by the frequency domain analysis in Section 2.5, i.e., for the index set (18).

Let $V_{\mathcal{I}_q}$ be the matrix (21) for the index set \mathcal{I}_q . Likewise, let $\tilde{w}^{(q)}(t) \in \mathbb{R}^q$ be approximations of the coefficient functions (7) associated to basis functions determined by the index set \mathcal{I}_q . Assuming $q < k$, we achieve a least squares problem

$$\min_{\tilde{w}^{(q)}(t) \in \mathbb{R}^q} \left\| V_{\mathcal{I}_q} \tilde{w}^{(q)}(t) - \bar{y}(t) \right\|_2 \quad (27)$$

with the Euclidean norm $\|\cdot\|_2$ point-wise in time. Since the matrix $V_{\mathcal{I}_q}$ exhibits full rank, a unique solution $\check{w}^{(q)}$ exists. The solution $\check{w}^{(q)}$ directly yields a low-dimensional approximation (16).

Moreover, the matrix $V_{\mathcal{I}_q}$ is time-invariant and thus a QR -factorization, see [28, p. 246], of this matrix can be reused to solve the least squares problems in all time points. This property makes the technique also advantageous in the case of $q \approx k$ ($q < k$), if k is not too large. Using Householder transformations, the number of operations becomes $2kq^2 - \frac{2}{3}q^3$ in the QR -factorization. The numerical solution of the problem (27) with a given QR -decomposition requires just about $2kq + \frac{1}{2}q^2$ operations. Proceeding for $q = 1, \dots, q_{\max}$, rank-one updates can be used in the QR -decompositions, see [28, p. 334], for keeping the computational complexity small.

3.4 Related work

The goal of this paper is to explore methods for producing sparse representations of the output of linear dynamical systems. Specifically, we consider time-frequency analysis and compressive sensing to produce sparse representations. Other approaches do exist for reducing the complexity of a polynomial approximation of a function. For example, low-rank approaches [34, 17] can be used to find low-rank approximations of the coefficients of a tensor-product polynomial basis. For tensor-train representations [35], the number of unknowns grows only linearly with dimension and quadratically with rank. The coefficients of a tensor-product basis are often dense. However, there have been some attempts to combine low-rank approximation with sparsity inducing methods [36, 18].

The cardinality (8) of the total-degree polynomial basis grows exponentially with dimension d and, consequently, can become intractable for large number of variables. Often only a subset of variables and interactions between variables contribute significantly to variations in a function. The (adaptive) ANOVA decomposition can be used to identify and exploit such effective dimensionality [14, 15, 16]. A method that exploits both sparsity and adaptive ANOVA was developed in [37].

The ability to recover sparse, and even low-rank approximations, is dependent on the method used to select samples at which to evaluate the function being approximated. For sparse approximation using Legendre basis randomly sampling from the uniform probability measure, as we do in Section 4, is adequate. However, for other orthogonal polynomials sampling from the probability measure can dramatically decrease the ability to recover sparse approximations. Changes of measure have been used successfully to improve

sparse recovery [38, 39, 40]. Algorithms for generating samples with a well-conditioned Vandermonde matrix via subsampling of tensor-product quadrature have also been used for sparse approximation [41] as well as regression, interpolation and low-rank approximation [42, 43, 44, 45].

3.5 Error measures in time domain

We assume that the solution of the stochastic Galerkin system (9) yields a sufficiently accurate approximation (10) of the QoI by the selection of a sufficiently large total degree d . Thus the truncation error as well as the error of the Galerkin approach are negligible in comparison to a sparsification error. A low-dimensional approximation (16) is defined by the index set \mathcal{I} and its coefficient functions \tilde{w}_i for $i \in \mathcal{I}$. We embed these coefficients in a vector $\tilde{w} \in \mathbb{R}^m$ by specifying $\tilde{w}_i = 0$ for $i \notin \mathcal{I}$.

In the time domain, the $\mathcal{L}^2(\Pi, \rho)$ -norm (4) of the error becomes

$$\left\| \hat{y}^{(m(d))}(t, \cdot) - \tilde{y}^{(\mathcal{I})}(t, \cdot) \right\|_{\mathcal{L}^2(\Pi, \rho)} = \|\hat{w}(t) - \tilde{w}(t)\|_2 \quad \text{for } t \geq 0$$

with the Euclidean norm $\|\cdot\|_2$ due to Parseval's theorem. We examine the relative error in $\mathcal{L}^2(\Pi, \rho)$, i.e.,

$$E_{\mathcal{L}^2}(t) := \frac{\|\hat{w}(t) - \tilde{w}(t)\|_2}{\|\hat{w}(t)\|_2} \quad (28)$$

point-wise for $t \geq 0$.

The identification of low-dimensional representations uses k samples (19) of the QoI. Both the minimization problem from Section 3.2 and the least squares problem from Section 3.3 feature the property that the residual (25) decreases monotone for increasing dimension q of the subspace at fixed time. The residual (25) also yields a rough estimate of the $\mathcal{L}^2(\Pi, \rho)$ -norm of the difference between the exact QoI and the low-dimensional representation, i.e.,

$$\left\| y(t, \cdot) - \tilde{y}^{(\mathcal{I})}(t, \cdot) \right\|_{\mathcal{L}^2(\Pi, \rho)} \approx \frac{1}{\sqrt{k}} \|V\tilde{w}(t) - \bar{y}(t)\|_2 \quad (29)$$

for each t . The estimate (29) converges for $k, m \rightarrow \infty$ in probability (provided that the orthonormal basis is complete).

The error measures (28) and (25) are given point-wise in time. Global measures can be obtained by taking (integral) mean values on a finite time interval. In practice, the problems are solved for a finite set of time points and (arithmetic) means can be applied.

4 Test Example

We use a mass-spring-damper system from [46] depicted in Figure 1. This configuration consists of 4 masses, 6 springs and 4 dampers, i.e., $n_{\text{par}} = 14$ parameters. The input is the excitation at the bottom mass, whereas the position of the top mass represents the output. The mathematical modeling yields a system (1) of ODEs with dimension $n = 8$.

Transient simulations are performed in a time interval $[0, T]$. We supply a harmonic oscillation as input signal

$$u(t) = \begin{cases} \sin(\omega_0 t) & \text{for } 0 \leq t \leq T, \\ 0 & \text{otherwise,} \end{cases} \quad (30)$$

with frequency ω_0 . The compact support $[0, T]$ guarantees $u \in \mathcal{L}^2[0, \infty)$. We choose $T = 500$ and $\omega_0 = 0.1$ in this test example. It holds that $\|u\|_{\mathcal{L}^2[0, \infty)} \approx 16$.

In the following, all IVPs of ODEs are solved numerically by a Runge-Kutta method of order 4(5) with a step size selection based on the relative tolerance $\varepsilon_{\text{rel}} = 10^{-6}$ and the absolute tolerance $\varepsilon_{\text{abs}} = 10^{-8}$. These high accuracy requirements imply that the errors of the time integrations are negligible in comparison to the other error sources.

In the stochastic modeling, we choose the means of parameters as the values given in [46]. Independent uniformly distributed random variables are introduced with 5% variation around the mean values. Thus the

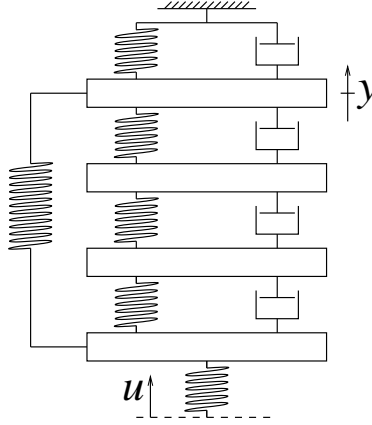


Figure 1: Mass-spring-damper configuration.

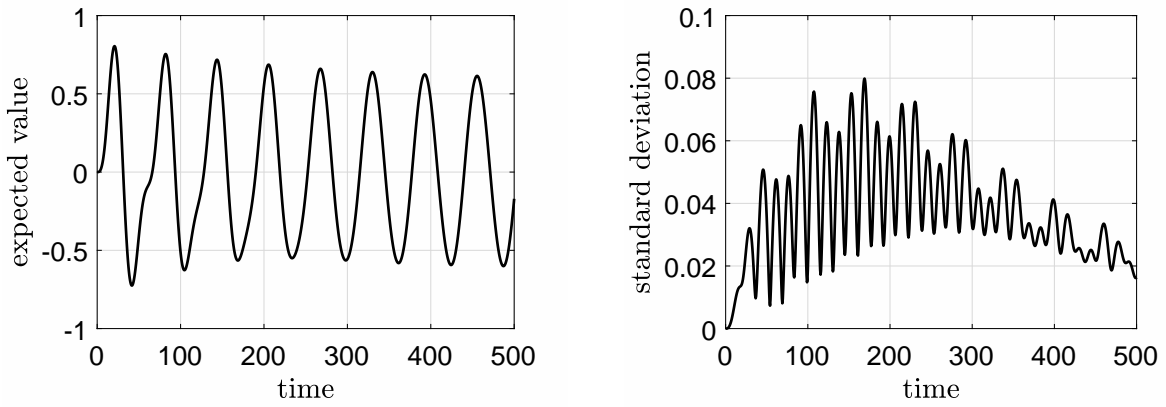


Figure 2: Expected value (left) and standard deviation (right) of random output for periodic input signal in mass-spring-damper system.

gPC expansions (6) include the multivariate Legendre polynomials. We incorporate all polynomials up to total degree $d = 3$, which results in $m = 680$ basis functions: 1 of degree zero, 14 of degree one, 105 of degree two and 560 of degree three.

Now we arrange the stochastic Galerkin system (9) of dimension $mn = 5440$. The spectral abscissa (largest real part of eigenvalues in matrix pencil $\lambda\hat{E} - \hat{A}$) becomes -0.0049 , which confirms the asymptotic stability of the linear dynamical system. We solve the IVP with the input (30). The numerical solution yields approximations of the expected value as well as the standard deviation with respect to the QoI. Figure 2 illustrates these statistics.

The quadrature technique produces approximations of the \mathcal{H}_2 -norms (13) as described in Section 2.3.2. We choose $\omega_{\min} = 10^{-2}$ and $\omega_{\max} = 10^2$. In the interval $[\omega_{\min}, \omega_{\max}]$, we use a logarithmically spaced grid with $\nu = 200$ points. Broader intervals $[\omega_{\min}, \omega_{\max}]$ or higher numbers of grid points do not considerably change the results. The computed norms are shown in Figure 3. We observe that the norms exhibit different orders of magnitudes and a rapid decay. The \mathcal{H}_2 -norms allow for the computation of the error bounds in the right-hand side of (17) using the optimal index sets (18) for increasing dimensions. Figure 4 depicts the error estimates for a normalized input, i.e., $\|u\|_{\mathcal{L}^2[0,\infty)} = 1$. Even though the error bounds are not sharp, they decrease exponentially.

Furthermore, we generate $k = 500$ samples of the QoI by solving IVPs of the linear dynamical system (1) with input (30) in the interval $[0, T]$. We determine low-dimensional representations (16) in equidistant time points $t_j = j\frac{T}{r}$ for $j = 1, \dots, r$ using $r = 1000$. The presented results are arithmetic mean values of the

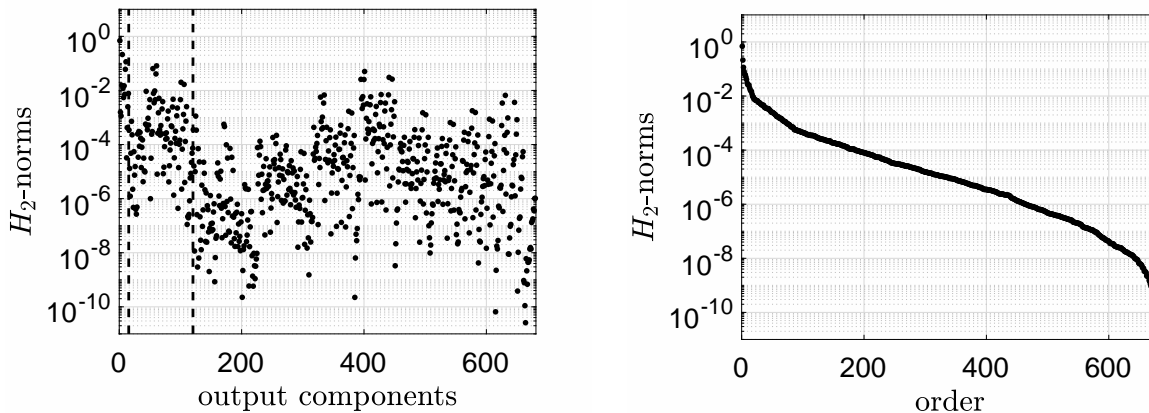


Figure 3: \mathcal{H}_2 -norms of output components in stochastic Galerkin system: for each component (left), dashed lines separate the coefficients for polynomial degree zero/one, two and three, and in descending order (right).

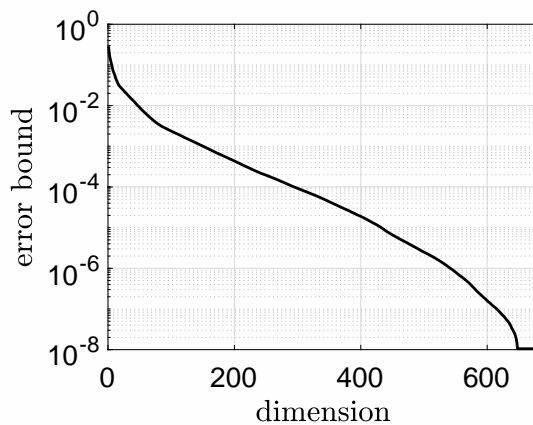


Figure 4: Optimal error bounds (17) from \mathcal{H}_2 -norms for input with unit norm given different dimensions of subspaces (number of basis polynomials).

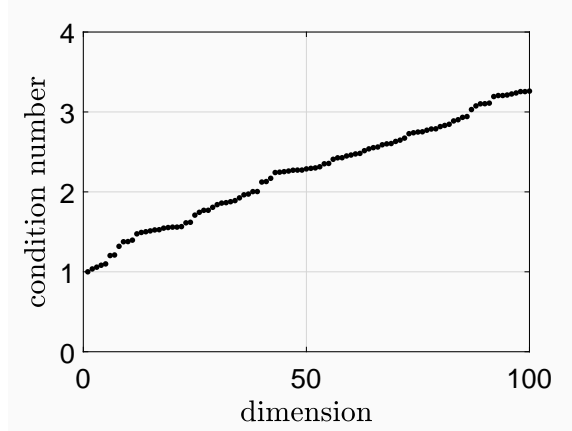


Figure 5: Condition numbers of matrices in linear least squares problems (27) for different dimensions.

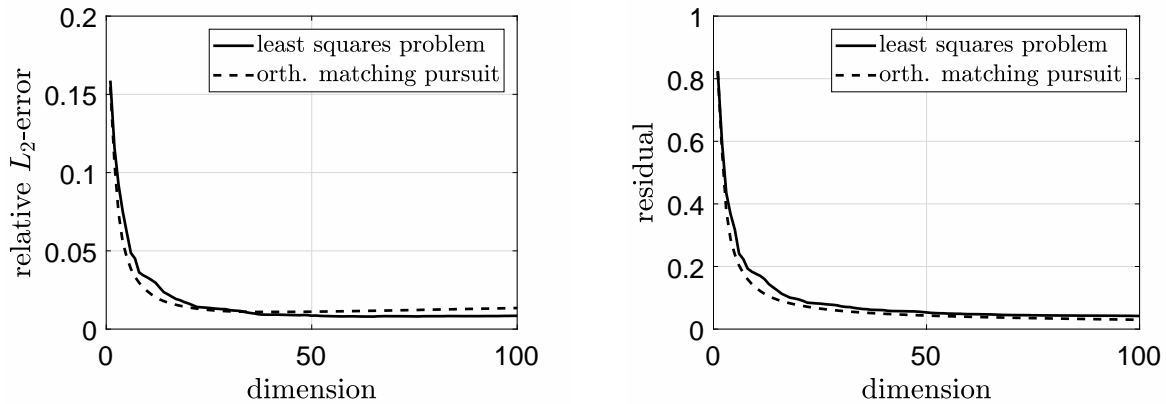


Figure 6: Relative \mathcal{L}^2 -errors (28) (left) and residuals (25) (right) of the low-dimensional representations obtained by least squares problem and OMP approach.

quantities in these time points, which can be seen as approximations of an integral mean.

We compute q -sparse approximations (16) for $q = 1, 2, \dots, 100$. On the one hand, the least squares problems from Section 3.3 are solved, where the frequency domain analysis yields the sequence of bases. The subspace of dimension q is time-invariant in this approach. Figure 5 shows the condition numbers (with respect to the spectral norm) of the matrices in the least squares problems (27). We observe that all problems are well-conditioned. On the other hand, the minimization problem including OMP from Section 3.2 is applied, where the basis selection takes place separately for each time point. Concerning the \mathcal{L}^2 -error, the transient solution of the Galerkin-projected system (9) serves as reference solution in the r time points. Figure 6 demonstrates both \mathcal{L}^2 -errors (28) and residuals (25). The residuals decrease monotone in both methods, which is guaranteed point-wise in time by construction. The \mathcal{L}^2 -errors of the least squares problem also reduce monotone for increasing dimensions of the subspaces. In the OMP technique, this error decreases rapidly first and then increases slightly. The reason is that the underlying minimization problem (22) with $\varepsilon = 0$ tends to an interpolation of the samples for higher dimensions of the subspaces.

For fixed dimension q , we obtain index sets $\mathcal{I}_q^{\text{lsP}}$ and $\mathcal{I}_q^{\text{OMP}}$ from the two techniques, which are associated to subsets of basis polynomials. It holds that $|\mathcal{I}_q^{\text{lsP}}| = |\mathcal{I}_q^{\text{OMP}}| = q$. We investigate the agreement of the two sets. The ratio of basis functions in the intersection reads as

$$\theta(q) := \frac{|\mathcal{I}_q^{\text{lsP}} \cap \mathcal{I}_q^{\text{OMP}}|}{q}.$$

A ratio $\theta(q) = 0$ implies that the two sets are disjoint, whereas a ratio $\theta(q) = 1$ represents identical sets. The

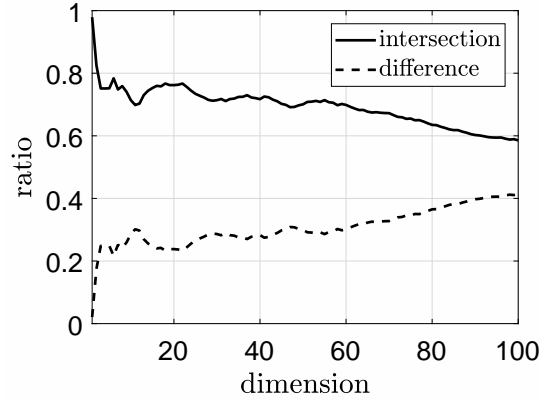


Figure 7: Ratio of basis polynomials in the intersection of index sets from least squares problem in Section 3.3 and sparse minimization problem in Section 3.2.

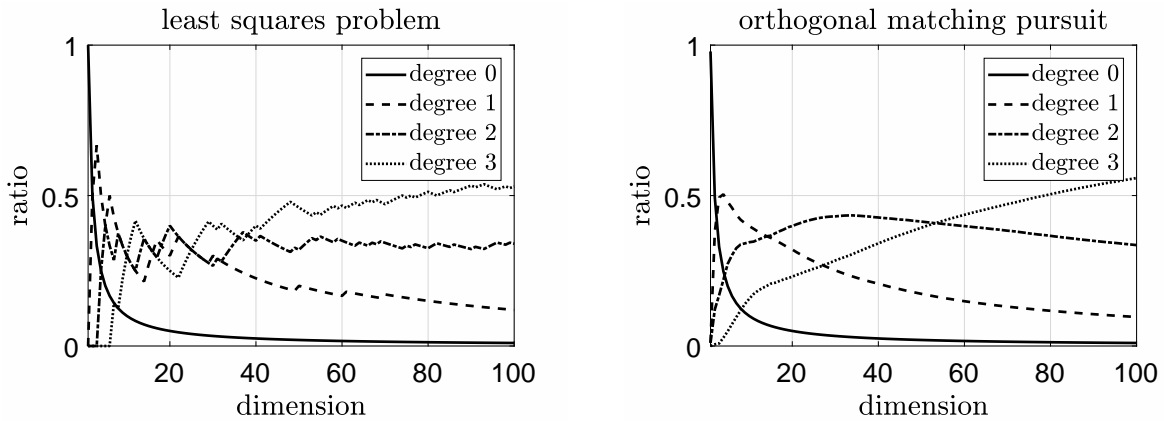


Figure 8: Ratios of the polynomials of different degrees in the subspaces identified by least squares problem from Section 3.3 (left) and sparse minimization problem from Section 3.2 (right).

larger the ratio the more the two basis selections agree. The value $1 - \theta(q)$ is the ratio for the differences $\mathcal{I}_q^{\text{ls}} \setminus \mathcal{I}_q^{\text{OMP}}$ as well as $\mathcal{I}_q^{\text{OMP}} \setminus \mathcal{I}_q^{\text{ls}}$. Figure 7 depicts these ratios, which represent the mean values in time again. We observe that about 60% or more of the basis functions are within both index sets for all dimensions. However, the relative \mathcal{L}^2 -error, see Figure 6, is nearly the same in both methods. The minimum errors are around 0.01, which can be seen as a good low-dimensional approximation. We conclude that basis polynomials in the intersection of both methods are the most important contributors to the approximation.

In addition, we examine the degrees of the polynomials within the index sets for the two methods separately. If q basis polynomials have been chosen in a method, then let q_j be the number of included polynomials of degree j ($0 \leq q_j \leq q$). We obtain the ratios $0 \leq \frac{q_j}{q} \leq 1$ for $j = 0, 1, 2, 3$. The sum of the four ratios is equal to one. Figure 8 shows that these ratios are similar in both approaches. The polynomial of degree zero is included in nearly all computed bases. The two techniques are able to identify the dominant basis polynomials among all degrees.

5 Conclusions

We compared two numerical techniques for a basis selection to achieve low-dimensional approximations in polynomial chaos expansions. In the first approach the basis is identified by an analysis in the frequency domain followed by a least squares problem for coefficients in the time domain. The second approach solves

a sparse minimization problem using information in the time domain.

We tested the methods on a linear dynamical system modeling a mechanical configuration. The numerical results demonstrate that both techniques identify low-dimensional approximations of the same quality, i.e., with a sufficiently small relative \mathcal{L}^2 -error. Although the identification of the basis polynomials uses different approaches, most of the selected basis functions (60% or more) coincide in both methods at all times. Moreover, the number of basis polynomials for each degree separately is nearly the same.

Acknowledgements

Sandia National Laboratories is a multimission laboratory managed and operated by National Technology and Engineering Solutions of Sandia, LLC., a wholly owned subsidiary of Honeywell International, Inc., for the U.S. Department of Energy's National Nuclear Security Administration under contract DE-NA-0003525. The views expressed in the article do not necessarily represent the views of the U.S. Department of Energy or the United States Government. John Jakeman's work was supported by DARPA EQUiPS. The authors are indebted to Prof. Dr. Akil Narayan (University of Utah) for helpful discussions.

References

- [1] Sullivan, T.J., *Introduction to Uncertainty Quantification*, Springer, 2015.
- [2] Xiu, D., *Numerical methods for stochastic computations: a spectral method approach*, Princeton University Press, 2010.
- [3] Augustin, F., Gilg, A., Paffrath, M., Rentrop, P., and Wever, U., Polynomial chaos for the approximation of uncertainties: chances and limits, *Euro. Jnl. of Applied Mathematics*, **19**, pp. 149–190, 2008.
- [4] Ernst, O.G., Mugler, A., Starkloff, H.J., and Ullmann, E., On the convergence of generalized polynomial chaos expansions, *ESAIM: Mathematical Modelling and Numerical Analysis* **46**, pp. 317–339, 2012.
- [5] Pulch, R., Polynomial chaos for linear differential algebraic equations with random parameters, *Int. J. Uncertain. Quantif.*, **1**(3), pp. 223–240, 2011.
- [6] Pulch, R., Stochastic collocation and stochastic Galerkin methods for linear differential algebraic equations, *J. Comput. Appl. Math.*, **262**, pp. 281–291, 2014.
- [7] Hampton, J. and Doostan, A., Coherence motivated sampling and convergence analysis of least-squares polynomial regression, *Comput. Methods Appl. Mech. Eng.*, **290**, pp. 73–97, 2015.
- [8] Blatman, G. and Sudret, B., Adaptive sparse polynomial chaos expansion based on least angle regression, *J. Comput. Phys.*, **230**, pp. 2345–2367, 2011.
- [9] Conrad, P.R. and Marzouk, Y.M., Adaptive Smolyak pseudospectral approximations, *SIAM J. Sci. Comput.*, **35**(6), pp. A2643–A2670, 2013.
- [10] Doostan, A. and Owhadi, H., A non-adapted sparse approximation of PDEs with stochastic inputs, *J. Comput. Phys.*, **230**, pp. 3015–3034, 2011.
- [11] Yan, L., Guo, L., and Xiu, D., Stochastic collocation algorithms using ℓ_1 -minimization. *Int. J. Uncertain. Quantif.*, **2**(3), pp. 279–293, 2012.
- [12] Nair, P.B. and Keane, A.J., Stochastic reduced basis methods, *AIAA J.*, **40**, pp. 1653–1664, 2002.
- [13] Sachdeva, S.K., Nair, P.B., and Keane, A.J., Hybridization of stochastic reduced basis methods with polynomial chaos expansions, *Probabilistic Eng. Mech.*, **21**, pp. 182–192, 2006.
- [14] Prasad, A.K. and Roy, S., Accurate reduced dimensional polynomial chaos for efficient uncertainty quantification of microwave/RF networks, *IEEE Transactions on Microwave Theory and Techniques*, **65**(10), pp. 3697–3708, 2017.

- [15] Yang, X., Choi, M., Lin, G., and Karniadakis, G.E., Adaptive ANOVA decomposition of stochastic incompressible and compressible flows. *J. Comput. Phys.*, **231**(4): pp. 1587–1614, 2012.
- [16] Zhang, Z., Yang, X., Oseledets, I.V., Karniadakis, G.E., and Daniel, L., Enabling high-dimensional hierarchical uncertainty quantification by ANOVA and tensor-train decomposition, *IEEE Transactions on Computer-Aided Design of Integrated Circuits and Systems*, **34**(1), pp. 63–76, 2015.
- [17] Oseledets, I.V., Constructive representation of functions in low-rank tensor formats, *Constr. Approx.*, **37**(1), pp. 1–18, 2013.
- [18] Zhang, Z., Weng, T.W., and Daniel, L., Big-data tensor recovery for high-dimensional uncertainty quantification of process variations, *IEEE Transactions on Components, Packaging and Manufacturing Technology*, **7**(5), pp. 687–697, 2017.
- [19] Pulch, R., Model order reduction and low-dimensional representations for random linear dynamical systems, *Math. Comput. Simulat.*, **144**, pp. 1–20, 2018.
- [20] Pati, Y., Rezaiifar, R., and Krishnaprasad, P., Orthogonal matching pursuit: Recursive function approximation with applications to wavelet decomposition, in *Proceedings of the 27th Annual Asilomar Conference on Signals, Systems, and Computers*, pp. 40–44, 1993.
- [21] Antoulas, A., *Approximation of Large-Scale Dynamical Systems*, SIAM Publications, 2005.
- [22] Xiu, D. and Karniadakis, G.E., The Wiener-Askey polynomial chaos for stochastic differential equations, *SIAM J. Sci. Comput.*, **24**(2), pp. 619–644, 2002.
- [23] Pulch, R. and Augustin, F., Stability preservation in stochastic Galerkin projections of dynamical systems, arXiv:1708.00958, 2017.
- [24] Pulch, R., ter Maten, E.J.W., and Augustin, F., Sensitivity analysis and model order reduction for random linear dynamical systems, *Math. Comput. Simulat.*, **111**, pp. 80–95, 2015.
- [25] Pulch, R. and ter Maten, E.J.W., Stochastic Galerkin methods and model order reduction for linear dynamical systems, *Int. J. Uncertain. Quantif.*, **5**(3), pp. 255–273, 2015.
- [26] Hairer, E. and Wanner, G., *Solving Ordinary Differential Equations. Vol. 2: Stiff and Differential-Algebraic Equations*, 2nd ed., Springer, 1996.
- [27] Benner P. and Stykel, T., Model order reduction of differential-algebraic equations: a survey, in *Surveys in Differential-Algebraic Equations IV*, A. Ilchmann and T. Reis, Eds., Differential-Algebraic Equations Forum, Springer, pp. 107–160, 2017.
- [28] Golub, G.H. and van Loan, C.F., *Matrix Computations*, 4th ed., Johns Hopkins University Press, 2013.
- [29] Sturm, B.L. and Christensen, M.G., Comparison of orthogonal matching pursuit implementations, in *Proceedings of the 20th European Signal Processing Conference (EUSIPCO)*, pp. 220–224, 2012.
- [30] Candes, E.J., Romberg, J.K., and Tao, T., Stable signal recovery from incomplete and inaccurate measurements, *Comm. Pure Appl. Math.*, **59**(8), pp. 1207–1223, 2006.
- [31] Rauhut, H., Compressive sensing and structured random matrices, in *Theoretical Foundations and Numerical Methods for Sparse Recovery*, M. Fornasier, Ed., **9**, DE GRUYTER, pp. 1–92, 2010.
- [32] Cai, T.T. and Wang, L., Orthogonal matching pursuit for sparse signal recovery with noise, *IEEE Trans. Inf. Theory*, **57**(7), pp. 4680–4688, 2011.
- [33] Kunis, S. and Rauhut, H., Random sampling of sparse trigonometric polynomials, II. orthogonal matching pursuit versus basis pursuit, *Found. Comput. Math.*, **8**(6), pp. 737–763, 2008.
- [34] Doostan, A., Validi, A., and Iaccarino, G., Non-intrusive low-rank separated approximation of high-dimensional stochastic models, *Comput. Methods Appl. Mech. Eng.*, **263**, pp. 42–55, 2013.

-
- [35] Gorodetsky, A.A. and Jakeman, J.J., Gradient-based optimization for regression in the functional tensor-train format, arXiv:1801.00885v2, accepted *J. Comp. Phys.*, 2018.
- [36] Mathelin, L., Quantification of uncertainty from high-dimensional scattered data via polynomial approximation, *Int. J. Uncertain. Quantif.*, **4**(3), pp. 243–271, 2014.
- [37] Jakeman, J.D., Eldred, M.S., and Sargsyan, K., Enhancing ℓ_1 -minimization estimates of polynomial chaos expansions using basis selection, *J. Comput. Phys.*, **289**, pp. 18–34, 2015.
- [38] Hampton, J. and Doostan, A., Compressive sampling of polynomial chaos expansions: Convergence analysis and sampling strategies, *J. Comput. Phys.*, **280**, pp. 363–386, 2015.
- [39] Jakeman, J.D., Narayan, A., and Zhou, T., A generalized sampling and preconditioning scheme for sparse approximation of polynomial chaos expansions, *SIAM J. Sci. Comput.*, **39**(3), pp. A1114–A1144, 2017.
- [40] Rauhut, H. and Ward, R., Sparse Legendre expansions via ℓ_1 -minimization, *J. Approx. Theory*, **164**(5), pp. 517–533, 2012.
- [41] Tang, G. and Iaccarino, G., Subsampled Gauss quadrature nodes for estimating polynomial chaos expansions, *SIAM/ASA J. Uncertainty Quantification*, **2**(1), pp. 423–443, 2014.
- [42] Ahadi, M. and Roy, S., Sparse linear regression (spliner) approach for efficient multidimensional uncertainty quantification of high-speed circuits, *IEEE Transactions on Computer-Aided Design of Integrated Circuits and Systems*, **35**(10), pp. 1640–1652, 2016.
- [43] Li, H. and Zhang, D., Probabilistic collocation method for flow in porous media: Comparisons with other stochastic methods, *Water Resour. Res.*, **43**(9), W09409, 2007.
- [44] Manfredi, P., Vande Ginste, D., De Zutter, D., and Canavero, G.G., Generalized decoupled polynomial chaos for nonlinear circuits with many random parameters, *IEEE Microwave and Wireless Components Letters*, **25**(8), pp. 505–507, 2015.
- [45] Zhang, Z., El-Moselhy, T.A., Elfadel, I.M., and Daniel, L., Stochastic testing method for transistor-level uncertainty quantification based on generalized polynomial chaos, *IEEE Transactions on Computer-Aided Design of Integrated Circuits and Systems*, **32**(10), pp. 1533–1545, 2013.
- [46] Lohmann, B. and Eid, R., Efficient order reduction of parametric and nonlinear models by superposition of locally reduced models, in: *Methoden und Anwendungen der Regelungstechnik*, G. Roppenecker and B. Lohmann, Eds., Shaker, 2009.